International Journal of Heat and Mass Transfer 52 (2009) 4195–4202

Contents lists available at ScienceDirect

International Journal of Heat and Mass Transfer

journal homepage: www.elsevier.com/locate/ijhmt

A numerical and experimental investigation of different containers and PCM options for cold storage modular units for domestic applications

K.A.R. Ismail *, R.I.R. Moraes

Department of Thermal and Fluids Engineering, Faculty of Mechanical Engineering, State University of Campinas, UNICAMP, P.O. Box 6122, CEP 13083-970, Campinas (SP), Brazil

ARTICLE INFO

Article history:
Received 7 April 2008
Received in revised form 16 April 2009
Accepted 16 April 2009
Available online 6 June 2009

Keywords:
Solidification
Spherical capsules
PCM
Latent heat storage
Recycled cans
Recycled water bottles

ABSTRACT

This paper presents the results of an experimental and numerical study on the solidification of different phase change materials (PCM) encapsulated in spherical and cylindrical shells of different materials and diameters subject to constant surface temperature. The main objective is to determine the time for complete solidification of the PCM and how it is affected by the variations of the surface temperature, material and diameter of spherical shells. As a result of the study, it is expected to define a pair of container and PCM to operate adequately and efficiently together with refrigeration units. The experiments were realized using glass and plastic spherical shells of diameters 0.035, 0.076, 0.106 and 0.131 m, soft drink cans and small plastic water bottles with surface temperatures of −5, −10, −12, −15, −18, −20 and −25 °C. The phase change materials used are water and mixtures of water with 3.75%, 7.5%, 15%, 25%, 30%, 40% and 50% Glycol content. The results are presented and discussed.

1. Introduction

The effective utilization of time varying energy resources depends essentially upon adequate and efficient energy storage methods capable of matching the energy supplies to energy demands. Three basic concepts are generally used for thermal energy storage, sensible heat storage, latent heat storage and hybrid energy storage. Sensible heat storage is well dominated technically with many operational installations all over the world. This type of storage has some intrinsic difficulties such as low energy density and temperature variation during the discharge and discharge processes. The literature is extremely rich with latent heat storage studies and reports on modeling, systems thermal analysis and applications. These systems are highly attractive because of their inherent high storage capacity and their nearly isothermal performance during the charging and discharging processes, but they suffer from poor heat transfer rate during the charging and discharging modes. The hybrid system combines sensible and latent heat strategies, attenuates the difficulties and incorporates some advantages of both concepts.

A lot of research work is reported on latent heat storage thermal modeling, experimental studies and performance analysis as in chapter 8 in Dincer and Rosen [1] and Ismail [17,18]. Some interesting numerical investigations were realized by Formin and Saitoh [2] who investigated the close contact melting within a spherical capsule. Their complete mathematical model was solved by the method of boundary fixing. An approximate approach was developed by Bareiss and Beer [3]. The predictions were validated against numerical results and agreements within 10–15% were reported. Caldwell and Chan [4] applied a numerical scheme based on the enthalpy method to the problem of solidification in spherical geometry and compared their results with the heat balance integral method. They concluded that the two methods agree well enough except when the Stefan number is very small. Ismail and Henriquez [5] realized a numerical study on the solidification of PCM inside a spherical capsule. Their mathematical model is based upon pure conduction and the boundary conditions of constant wall temperature and convection boundary condition on the external surface of the spherical shell were considered. Their numerical predictions were validated against available results and satisfactory agreement was reported. Khodadadi and Zhang [6] realized a numerical study to investigate the effects of buoyancy driven convection on constrained melting of PCM within spherical capsules. Their computational code is based upon iterative, finite volume numerical scheme in terms of primitive dependent variable. They found that buoyancy driven convection accelerates the melting process and that the Prandtl number in the range investigated from, 0.05 to 50, plays an important role during the melting process. Eames and Adref [7] realized experimental study on spherical capsules and obtained an empirical correlation to predict the solid fraction within the spherical shell. In their paper Barba and Spiga [8] analyzed the behavior of encapsulated PCM in three different geometries, plane, cylindrical and spherical for possible application

* Corresponding author. Tel.: +55 19 35213376; fax: +55 19 32893722.
E-mail address: kamal@fem.unicamp.br (K.A.R. Ismail).

0017-9310/$ - see front matter © 2009 Elsevier Ltd. All rights reserved.
doi:10.1016/j.ijheatmasstransfer.2009.04.031

Nomenclature

A	area (m^2)
Bi	Biot number ($=hr_i/\kappa$)
C_p	specific heat ($J\,kg^{-1}\,K^{-1}$)
h	convective heat transfer ($W\,m^{-2}\,K^{-1}$)
L	latent heat ($J\,kg^{-1}$)
M_{sol}	solidified mass (kg)
M_{total}	total mass (kg)
Q	heat flux (W)
r_f	position front (m)
r_i	internal shell radius (m)
r_e	external shell radius (m)
R_s	solid resistance (m^2 K/W)
R_h	convective resistance (m^2 K/W)
R_{esf}	spherical resistance (m^2 K/W)
$s(t)$	interface position (m)
Ste	Stefan number, $C(T_f - T_\infty)/L$
t	time (s)
T_f	temperature front (K)
T_∞	external surface temperature (K)
T_m	temperature phase change (K)
T_{sol}	solid temperature (K)
T_{liq}	liquid temperature (K)
T_i	internal temperature (K)
T_e	external temperature (K)

Greek symbols

α	thermal diffusivity, $\kappa/(\rho C)$ ($m^2\,s^{-1}$)
κ	thermal conductivity ($W\,m^{-1}\,K^{-1}$)
ρ	density ($kg\,m^{-3}$)
τ	dimensionless time

Subscripts

liq	liquid
m	phase change
sol	solid
sph	spherical

in domestic storage tanks. Their results show the influence of geometry and Jacob number on the time for complete solidification, and they concluded that the shortest time for complete solidification is obtained for small spherical shells with high Jacob number and high thermal conductivity. Ismail et al. [9] reported the results of a numerical investigation on the heat transfer during the solidification of water inside a spherical capsule. Their model and the associated boundary and initial conditions were formulated and solved by the finite difference approach and a moving grid scheme. The numerical predictions were validated against the experimental results. They investigated the effects of capsule size, the PCM and its initial, temperature and the external surface temperature of the capsule, on the solidified mass fraction, and the time for complete solidification. Bilir and Ilken [10] studied the inward solidification of PCM in spheres and cylinders. Kouskson et al. [11] investigated an industrial storage system with PCM encapsulated in spherical shells, examined the super-cooling phenomenon which delays crystallization of the PCM, developed a model and compared the numerical predictions with experiments. Wei et al. [12] conducted experimental and theoretical study on rapid heat release. In their numerical studies they analyzed four different encapsulating geometries (sphere, cylinder, plate and tube) and compared their results with experiments and found agreement within 10%. Hammou and Lacroix [13] proposed a hybrid thermal energy storage system to manage simultaneously the storage of solar heat and electric energy during off peak periods. Yuksel et al. [14] proposed a theoretical approach to represent the latent heat storage system during charging and discharging and their numerical predictions seem to agree well with available experimental data. Ettouney et al. [15] realized an experimental study on spherical shells filled with PCM and some metallic beads to determine the effect of the metallic beads on the enhancement of heat transfer within the spherical shell. Their results showed a reduction of about 15% in the time for melting and solidification and similar increase in the heat stored in the spherical shells. Assis et al. [16] presented a parametric study both numerically and experimentally on the melting of PCM in spherical shells. They realized their numerical simulation using Fluent 6.0 and compiled their experimental data to obtain a correlation for the prediction of the melt fraction in terms the Stefan, Grashoff and Fourier numbers.

This paper presents the results of a numerical and experimental study to evaluate the suitability of different options for encapsulating PCM for cold storage modular unit intended for domestic applications. Spherical glass and plastic capsules, metal and plastic cans were also investigated because of their abundance, low cost and their ambient impact. The experimental tests included various PCM to operate over a wide range of working temperatures with the objective of determining the time for complete solidification necessary to design of the proposed cold storage domestic unit and other applications.

2. Formulation of the problem

The solidification problem in the interior of a spherical shell is shown in Fig. 1, where the PCM is confined in the spherical shell of external radius r_e and internal radius r_i subject to an external surface temperature T_∞ lower than the phase change temperature T_f.

The heat transfer between the surrounding working fluid and the external surface is by convection where the heat transfer coefficient is constant and equal to h.

Consider that there is no internal energy generation, constant thermophysical properties, the heat transfer in the PCM is controlled by pure conduction and pure PCM. Based upon these

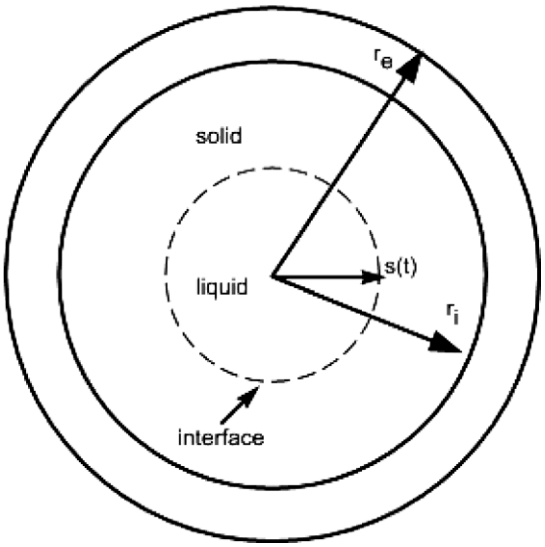

Fig. 1. Layout of the problem.

assumptions the heat conduction equation in spherical coordinates can be written as

$$\frac{\partial T}{\partial t} = \alpha\left[\frac{2}{r}\frac{\partial T}{\partial r} + \frac{\partial^2 T}{\partial r^2}\right] \quad 0 < r < r_i \tag{1}$$

As can be seen from Fig. 3, during the solidification process the solid and liquid phases coexist and are separated by an interface. Considering that the heat conduction equation controls the heat transfer process in both phases, one can write for the liquid domain

$$\frac{\partial T_{liq}}{\partial t} = \alpha_{liq}\left[\frac{2}{r}\frac{\partial T_{liq}}{\partial r} + \frac{\partial^2 T_{liq}}{\partial r^2}\right] \quad 0 \leqslant r \leqslant r_f \tag{2}$$

and for the solid domain

$$\frac{\partial T_{sol}}{\partial t} = \alpha_{sol}\left[\frac{2}{r}\frac{\partial T_{sol}}{\partial r} + \frac{\partial^2 T_{sol}}{\partial r^2}\right] \quad r_f < r \leqslant r_i \tag{3}$$

The boundary conditions in this case are

$$\text{At } r = 0, \quad \frac{\partial T_{liq}}{\partial r} = 0 \tag{4}$$

$$\text{At } r = r_i, \quad -k_{sol}A\frac{\partial T_{sol}}{\partial r} = Q \tag{5}$$

$$\text{At } r = r_f, \quad T_{liq} = T_{sol} = T_f \tag{6}$$

and

$$-\left(-k_{liq}\frac{\partial T_{liq}}{\partial r}\right) + \left(-k_{sol}\frac{\partial T_{sol}}{\partial r}\right) = -\rho_{sol}L\frac{dr_f}{dt} \tag{7}$$

The boundary condition:

$$\text{At } r = r_i, \quad Q = -kA\left.\frac{\partial T}{\partial r}\right|_{r=r_1}$$

where Q is obtained from a heat balance using the thermal resistance model shown in Fig. 2.

$$Q = \frac{T_\infty - T_i}{\frac{1}{4\pi k_{sph}}\left(\frac{1}{r_i} - \frac{1}{r_e}\right) + \frac{1}{4\pi h r_e^2}} \tag{8}$$

$$Q = \frac{4\pi(T_\infty - T_i)}{\frac{1}{k_{sph}}\left(\frac{r_e - r_1}{r_e r_i}\right) + \frac{1}{h r_e^2}} \tag{9}$$

To start the calculations it is necessary to determine the first thin solidified layer during the first instants of solidification. Assuming that the heat exchanged between the external fluid and the capsule is the heat used to solidify the first thin layer, one can write the heat balance in the form

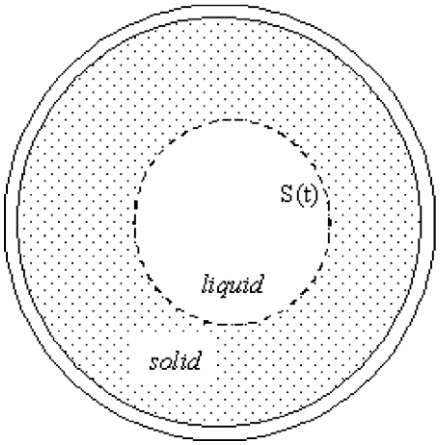

Fig. 3. The general case with the two phases present.

$$Q_f = -\rho L\frac{d\forall}{dt} = -4\pi\rho L r_f^2\frac{dr_f}{dt} \tag{10}$$

where Q_f is the heat delivered by the capsule, $d\forall$ is the volume of the solidified element and r_f is the position of the interface. The heat delivered by the capsule can be alternatively calculated by the thermal resistance circuit as indicated in Fig. 4 in the form

$$Q_f = \frac{T_f - T_\infty}{R_{sol} + R_{sph} + R_h} \tag{11}$$

where

$$R_{sol} = \frac{r_i - r_f}{4\pi k_{sol} r_i r_f} \tag{12}$$

$$R_{sph} = \frac{r_e - r_i}{4\pi k_{sph} r_i r_e} \tag{13}$$

$$R_h = \frac{1}{4\pi r_e^2 h} \tag{14}$$

Equating the two expressions for Q_f one can write

$$-4\pi\rho L r_f^2\frac{dr_f}{dt} = \frac{T_f - T_\infty}{\frac{r_i - r_f}{4\pi k_{sol} r_i r_f}} + \frac{r_e - r_i}{4\pi k_{sph} r_i r_e} + \frac{1}{4\pi r_e^2 h} \tag{15}$$

which after integration and performing some mathematical manipulations can be written as

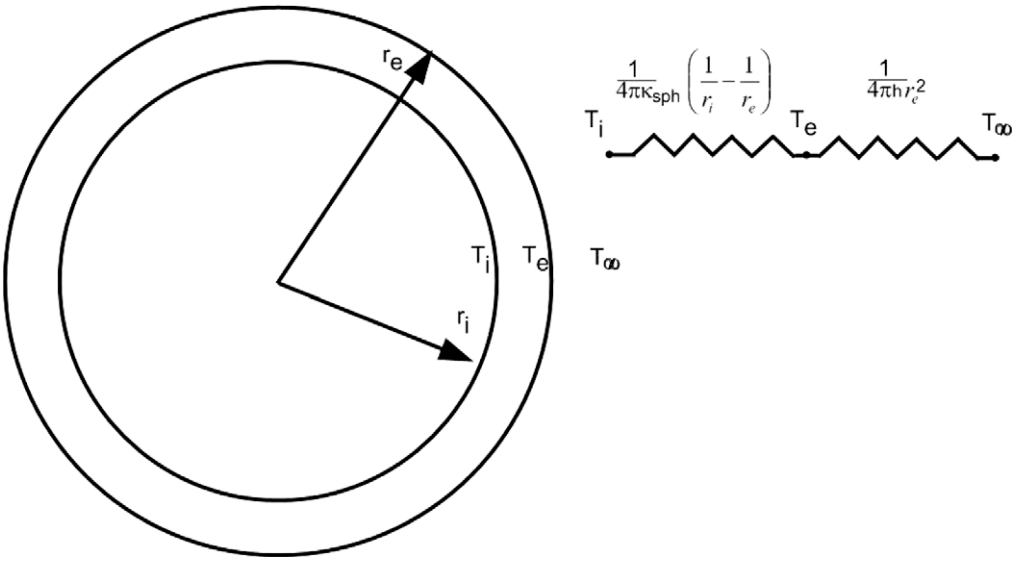

Fig. 2. Energy balance to determine the initial thin solid layer.

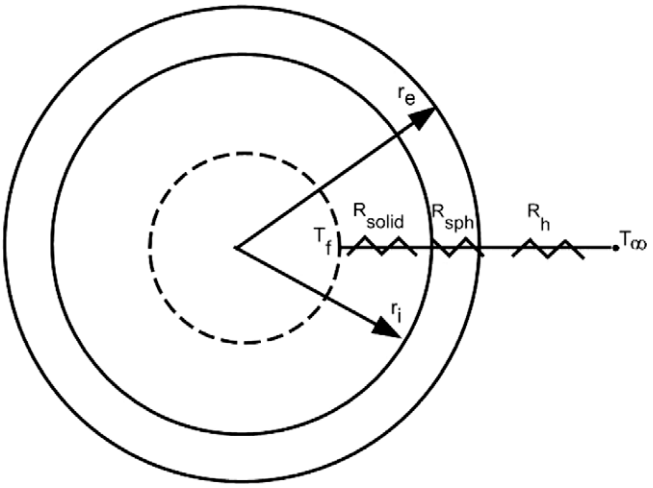

Fig. 4. Representation of the thermal resistance to calculate the first initial solidified layer.

$$\frac{r_f^2}{2r_i}-\frac{r_f^3}{3r_i^2}+\frac{k_{sol}}{3k_{sph}}\frac{r_f^3}{r_i^2}\left(\frac{r_e-r_i}{r_e}\right)+\frac{k_{sol}}{3hr_i}\frac{r_f^3}{r_e^2}+C=-\frac{(T_f-T_\infty)}{\rho L}\frac{k_{sol}}{r_i}t \tag{16}$$

This heat balance is valid only for the first instants, one can consider that as the time $t\to 0$, $r_f\to r_i$. Applying this condition to Eq. (9), one can determine the value of the constant C as

$$C=-\left[\frac{r_i}{6}+\frac{r_i}{3}\frac{k_{sol}}{k_{sph}}\left(\frac{r_e-r_i}{r_e}\right)+\frac{k_{sol}}{3hr_i}\frac{r_i^3}{r_e^2}\right] \tag{17}$$

Substitute the expression of C in Eq. (15) one can obtain

$$r_i\left[\frac{r_f^2}{2r_i^2}-\frac{r_f^3}{3r_i^3}+\frac{k_{sol}}{3k_{sph}}\frac{r_f^3}{r_i^3}\left(\frac{r_e-r_i}{r_e}\right)+\frac{k_{sol}}{3hr_i^2}\frac{r_f^3}{r_e^2}\right]-\left[\frac{r_i}{6}+\frac{r_i}{3}\frac{k_{sol}}{k_{sph}}\left(\frac{r_e-r_i}{r_e}\right)+\frac{k_{sol}}{3hr_i}\frac{r_i^3}{r_e^2}\right]=-\frac{(T_f-T_\infty)}{\rho L}\frac{k_{sol}}{r_i}t \tag{18}$$

Introducing a new variable $s(t)$, where $s(t)$ is the instantaneous interface position

$$s(t)=1-\frac{r_f}{r_i}\quad\text{or}\quad\frac{r_f}{r_i}=1-s(t) \tag{19}$$

Substituting Eq. (19) into Eq. (18) one can obtain

$$\left[\frac{(1-s(t))^2}{2}-\frac{(1-s(t))^3}{3}+\frac{k_{sol}}{3k_{sph}}(1-s(t))^3\left(\frac{r_e-r_i}{r_e}\right)+\frac{k_{sol}}{3hr_i}\frac{(1-s(t))^3}{r_e^2}r_i^2\right]-\left[\frac{1}{6}+\frac{1}{3}\frac{k_{sol}}{k_{sph}}\left(\frac{r_e-r_i}{r_e}\right)+\frac{k_{sol}}{3hr_i}\frac{r_i^3}{r_e^2}\right]=-\frac{(T_f-T_\infty)k_{sol}}{\rho L r_i^2}t \tag{20}$$

Introducing the following dimensionless parameters:

$$\tau=\frac{\alpha t}{r_i^2}\quad Bi=\frac{hr_i}{k_{sol}},\quad Ste=\frac{C_p(T_f-T_\infty)}{L}$$

into Eq. (20) one can write

$$\left[\frac{(1-s(t))^2}{2}-\frac{(1-s(t))^3}{3}+\frac{k_{sol}}{3k_{sph}}(1-s(t))^3\left(\frac{r_e-r_i}{r_e}\right)+\frac{1}{Bi}\frac{(1-s(t))^3}{3r_e^2}r_i^2\right]-\left[\frac{1}{6}+\frac{k_{sol}}{3k_{sph}}\left(\frac{r_e-r_i}{r_e}\right)+\frac{1}{3Bi}\frac{r_i^3}{r_e^2}\right]=-Ste\,\tau \tag{21}$$

or

$$\tau=\frac{1}{Ste}\left[\frac{1}{6}+\frac{1}{3Bi}\left(\frac{r_i}{r_e}\right)^2(1-(1-s(t))^3)+\frac{k_{sol}}{3k_{sph}}\left(1-(1-s(t))^3\right)\right]\cdot\left(\frac{r_e-r_i}{r_e}\right)-(1-s(t))^2\cdot\left[\frac{1}{2}-\frac{(1-s(t))}{3}\right] \tag{22}$$

At the beginning of the solidification process $s(t)\ll 1$ and Eq. (21) becomes

$$\tau=\frac{1}{Ste}\left(1-(1-s(t))^3\right)\cdot\left[\frac{1}{3Bi}\left(\frac{r_i}{r_e}\right)^2+\frac{k_{sol}}{3k_{sph}}\left(\frac{r_e-r_i}{r_e}\right)\right] \tag{23}$$

where τ is the dimensionless time.

The above model (Eqs. (2)–(9)) is represented by the finite difference approximation and the resulting equation and the associated boundary conditions were treated by using a moving grid method.

Numerical tests were realized to ensure that the results are independent of the grid size. The optimized parameters are found to be

The number of elements in the liquid phase $M = 50$.
The number of elements in the solid phase $N = 50$.
The time step = 1 s.

The above values were used in all the calculations. The solidified mass at any instant is calculated from

$$M_{sol,t}=\left[\frac{4}{3}\pi(r_i^3-r_f^3)\right]\rho_{sol} \tag{24}$$

Total solidified mass of the PCM,

$$M_{total}=\frac{4}{3}\pi r_i^3\rho_{sol} \tag{25}$$

The solidified mass fraction is

$$FM_t=\frac{M_{sol,t}}{M_{total}} \tag{26}$$

The numerical predictions from the present model are compared with experimental to establish the validity of the model and the numerical results. Reasonably good agreements were found as can be verified in Section 4.

3. Experimental setup

The experimental rig is composed of a thermally insulated square tank. The working fluid (ethanol) in the tank (2) is cooled by a Freon circuit fed by a refrigeration unit (not shown in Fig. 5). The temperature of the working fluid in the tank is controlled by an OMEGA temperature controller within ±1 °C. The capsule is filled with PCM and then a carefully calibrated thermocouple ±0.5 °C is placed at the center of the capsule as shown in Fig. 5.

The tests are realized as follows. The spherical shell is filled with the PCM, and the calibrated thermocouple is inserted at its center. The thermocouple is connected to the data acquisition system and to a PC. The secondary working fluid (ethanol) is then circulated into the coil until the ethanol in the tank reaches the required temperature. The spherical shell is then submersed into the tank and the test is initiated. The temperature at the center of the shell and the corresponding time are registered. When the temperature at the center reaches the pre-established value, the experiment is stopped and the equipment is turned off in order to prepare the experimental set up for the next test.

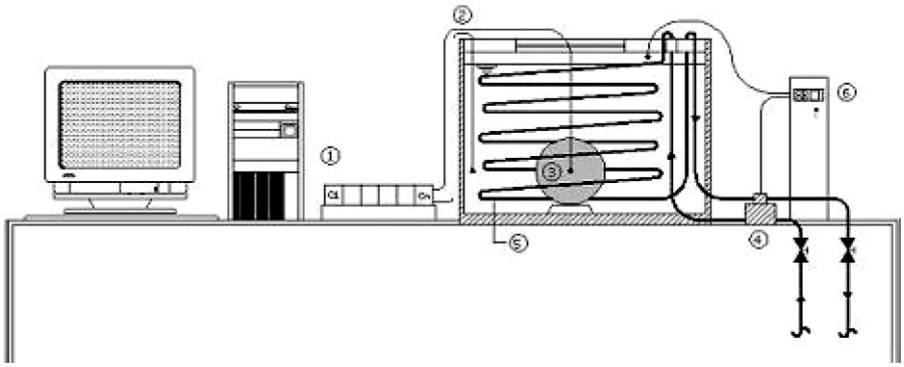

Fig. 5. Experimental rig. 1, data acquisition system; 2, thermocouple for bath temperature; 3, thermocouple for shell center; 4, refrigeration control; 5, cooling coil; 6, temperature control.

In the present study, the temperature of the working fluid was varied as follows: −5, −10, −12, −15, −18, −20, −25 °C and the diameters of spherical shells selected for the tests are 0.035, 0.076, 0.106 and 0.131 m. The PCM used is water and water Glycol mixtures of the following Glycol content 3.75%, 7.5%, 15%, 25%, 30%, 40%, and 50%. The tests were realized using spherical shells of different materials, soft drink metallic and plastic cans and bottles.

4. Results and discussion

4.1. Cooling curves of the spherical capsules

Fig. 6 shows the variation of the temperature at the center of the spherical capsule as a function of time for a typical spherical shell and comparison with the numerical predictions. One can observe that, except for the supercooling phenomenon, the experiments and the numerical predictions seem to be in good agreements. The curves show some super cooling just before the PCM starts to solidify, followed by a long solidification period until the solidification front reaches the shell center and then starts a period of sensible heat cooling. This behavior was observed during all the tests realized and hence confirm similar comments and observations due to other authors [11].

Fig. 7 shows similar behavior for the metallic soft drink cans with no super cooling and a big reduction in the time for complete solidification. Fig. 8 shows the results for the plastic water bottle indicating some supercooling.

4.2. Effect of varying the glycol content in the PCM

The phase change materials used in the tests are pure water and mixture of water and glycol of various glycol contents. The phase change temperatures of the glycol–water mixtures used in the tests were determined experimentally and the results are shown in Fig. 9. As can be seen the variation of the phase change temperature of the PCM mixture is nearly linear with the glycol content for the range considered. This linear relation is useful for rapid estimates of the phase change temperature of other intermediate mixtures.

Fig. 10 shows the effect of varying the PCM on the time for complete solidification. The glycol content in the mixtures tested is 7.5%, 15%, 30% and 50%. It is found that when the surface temperature is reduced the time for complete solidification is reduced.

Fig. 11 shows the variation of the time for complete solidification as a function of the glycol content in the PCM for working temperature of −5 °C for the case of the metallic soft drink can indicating the increase of the time for complete solidification as the Glycol content in the PCM is increased.

4.3. Effect of varying the diameter of the spherical shell

Fig. 12 shows the effect of varying the diameter of the spherical shell on the time for complete solidification. As can be seen, the time for complete solidification increases dramatically with the increase of the diameter of the shell. In the case of small spherical capsules up to 0.076 m, the variation of the solidification time with the increase of diameter and also with the variation of the temperature of the working fluid is relatively small. The dominant heat transfer mode in these cases is conduction. With the increase of the shell diameter convection currents grow stronger and the heat transfer is dominated by convection.

4.4. Effect of the working fluid temperature

Fig. 13 shows the experimental results for four spherical shells of different diameters subjected to different working fluid temperatures. As can be seen the time for complete solidification is marginally affected by working fluid temperature or the diameter of the capsule when the shell diameter is small (below 0.076 m). On the other hand, the effect on the time for complete solidification is dramatic in case of larger shells, 0.106 and 0.131 m diameters. This effect is relatively strong for cases of low working fluid temperatures.

4.5. Effect of the material of the encapsulating shell

To investigate the effect of the shell material ordinary glass spherical and plastic capsules were tested under the same working conditions, that is, the same PCM and the same working temperature. Fig. 14 shows the effect of varying the encapsulation material and the PCM on the time for complete solidification. As can be seen the time for the complete solidification in the case of glass shell is less than that for plastic shell, every thing else the same. This is basically because of the thermal conductivity of the material. Tests realized with metallic containers confirm these results.

In order to validate the numerical model additional experimental measurements were realized. Each experiment was repeated three times and the average values were plotted in Fig. 15. This figure shows a comparison between the interface position determined numerically and that obtained by experimental measurements for the case of plastic spherical shell. A relatively good agreement is found between the predicted interface position and the measurements confirming the validity of the numerical model.

As can be seen lowering the low working temperature leads to reducing the time for complete solidification.

Fig. 16 shows a comparison between the numerical predictions of the solidified mass fraction and the experimental measurements as affected by the diameter of the spherical shell. It is found that

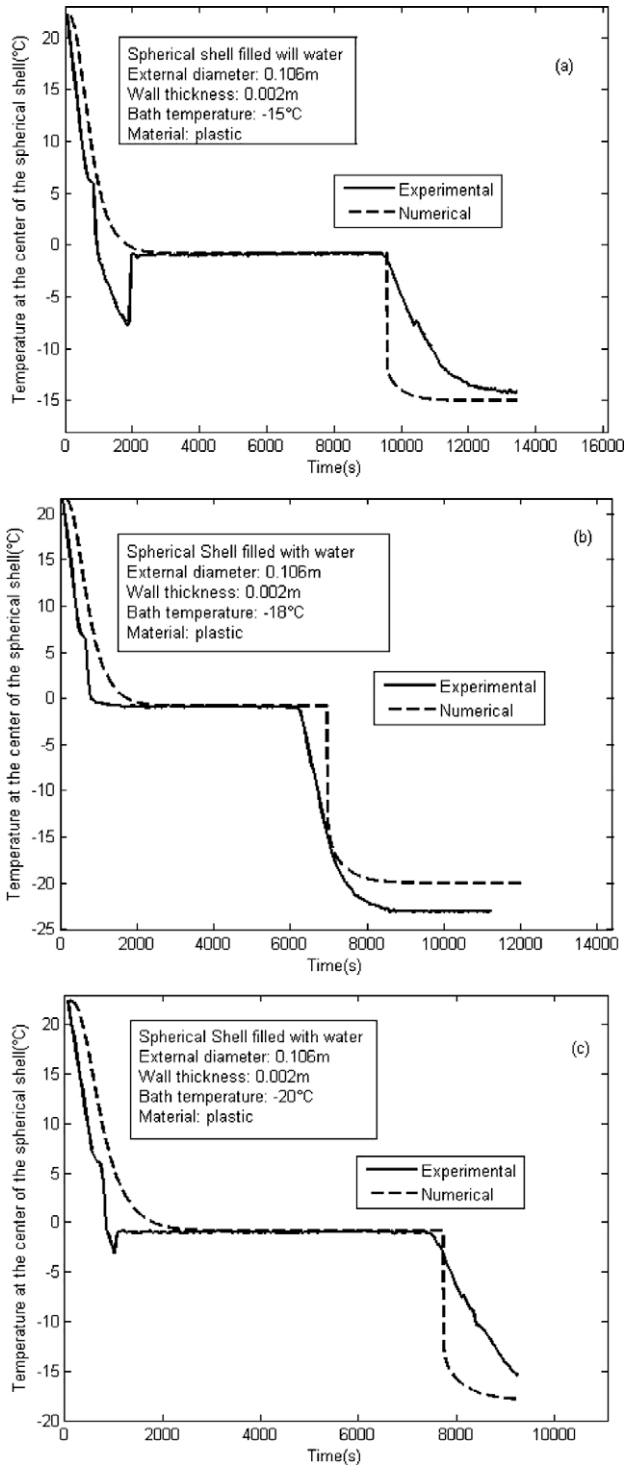

Fig. 6. Variation of temperature with time at the center of the spherical shell: (a), (b) and (c), diameter 0.106.

the increase of the shell diameter leads to increase of the time for complete solidification. One can also notice relatively good agreement between the numerical predictions and the experiments confirming the validity of the model.

5. Conclusions

Comparisons of the numerical predictions with the experimental measurements shows a relatively good agreement confirming the validity of the model.

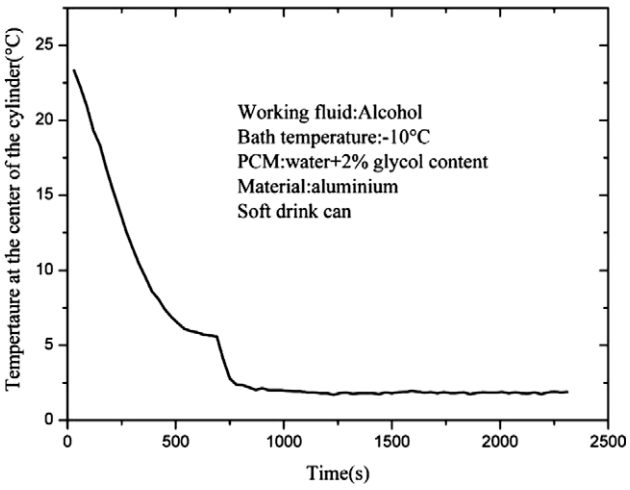

Fig. 7. Timewise variation of the PCM temperature at the center of soft drink can of 2% glycol content.

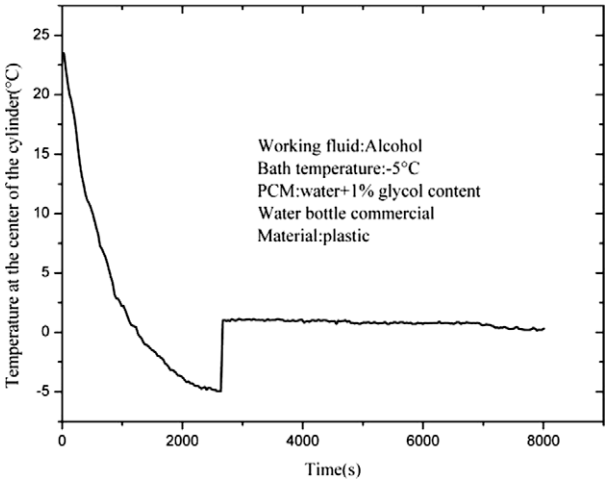

Fig. 8. Timewise variation of the PCM temperature at the center of water bottle.

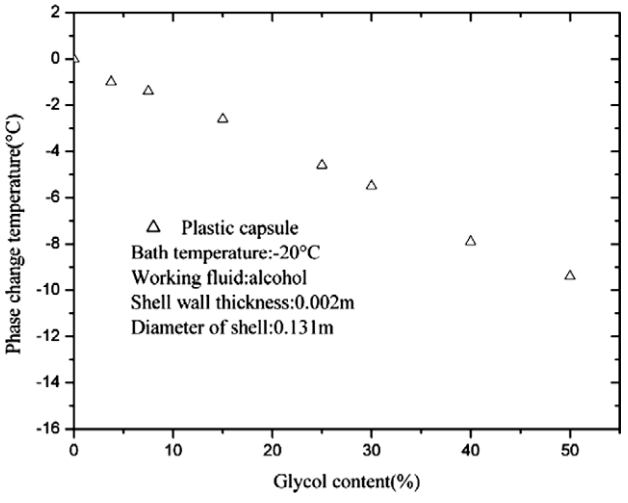

Fig. 9. Effect of varying the glycol content on the phase temperature of the PCM.

The solidification experiments indicated some super cooling just before the PCM starts to solidify in agreement with results

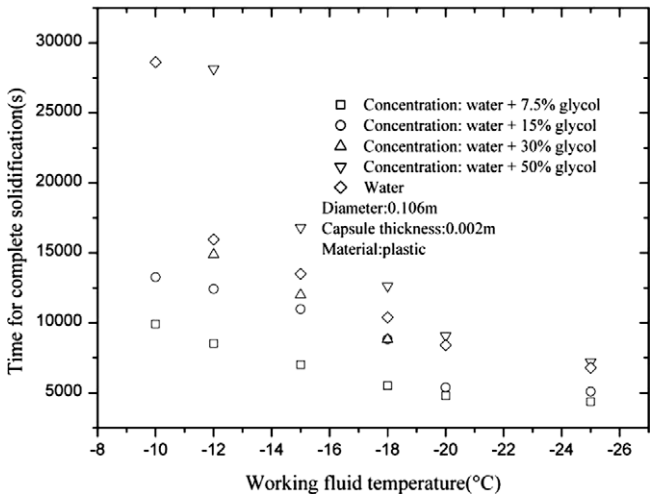

Fig. 10. Effect of variation of the glycol content and working fluid temperature on the time for complete solidification.

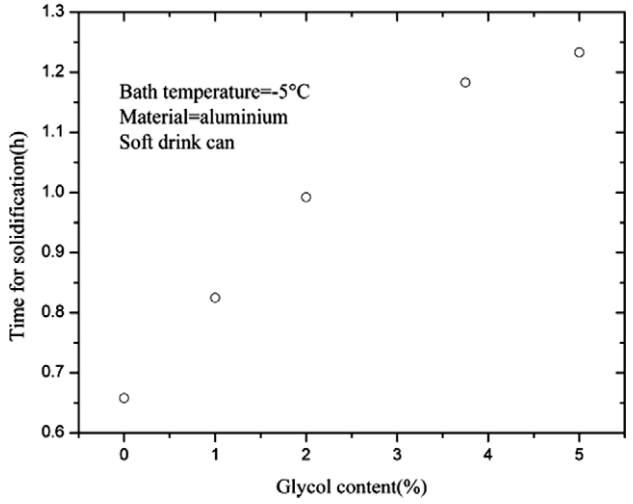

Fig. 11. Effect of the glycol content in the PCM on the time for complete solidification.

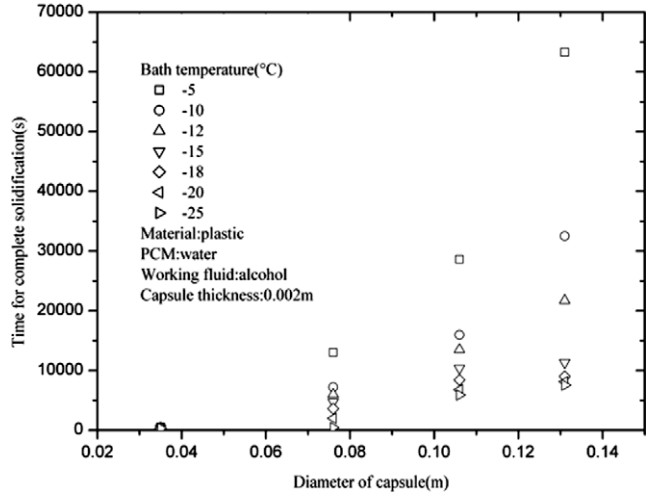

Fig. 12. Effect of varying the diameter of the spherical capsule on the time for complete solidification.

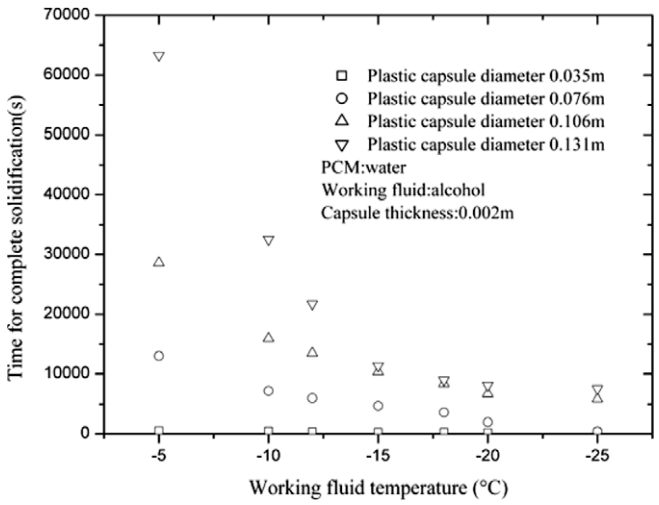

Fig. 13. Effect of varying the bath temperature on the time for complete solidification.

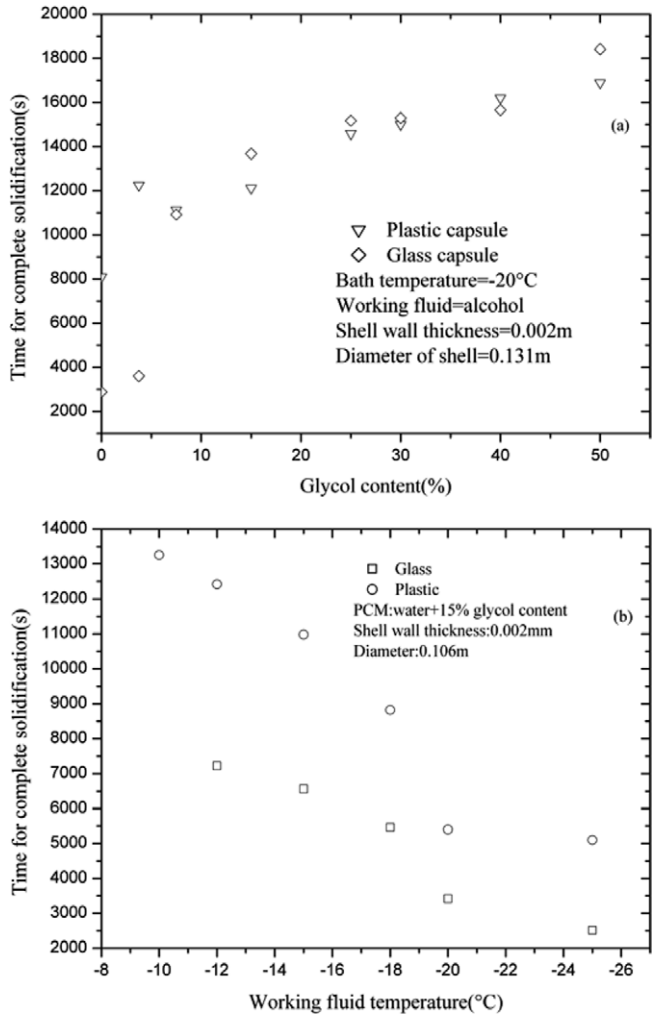

Fig. 14. Effect of the encapsulation material on the time for complete solidification: (a) effect of variation with the glycol content and (b) variation with the thermal conductivity.

and conclusions due to other authors. The increase of the glycol content in the mixture led to reducing the phase change temperature, reaching −15 °C when the Glycol content is 50%. It is also

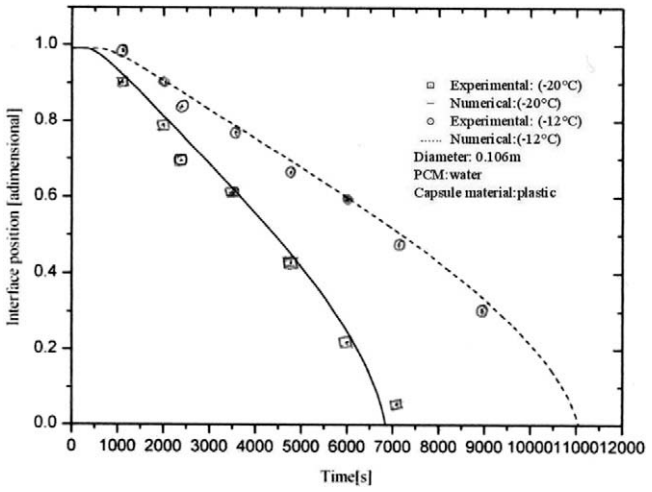

Fig. 15. Variation of the interface position with the working temperature experimentally and numerically.

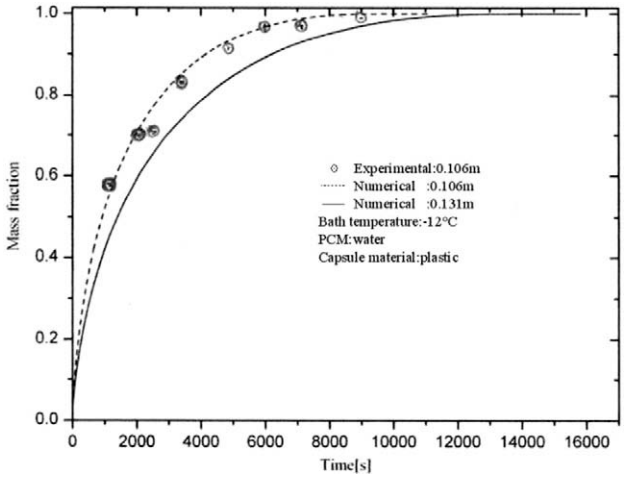

Fig. 16. Variation of the solidified mass fraction with the capsule size both experimentally and numerically.

found that the increase of Glycol content in the PCM led to increase the time for complete solidification for all working temperatures. The effect of increasing the diameter of the spherical shell is found to increase the time for complete solidification. Up to 0.076 m diameter, the increase is relatively small and in this case the dominant mode of heat transfer is conduction. As the diameter increases, convection in the liquid region moves the melt away from the solidifying front and hence increases the time for complete solidification.

As can be expected the working fluid temperature affects the solidification rate and hence the time for complete solidification. The reduction of the working temperature leads to reducing the time for complete solidification.

Tests realized with different shell materials indicated that encapsulating materials of high thermal conductivity reduce the time for complete solidification.

Acknowledgements

The authors wish to thank the National Research Council CNPQ for the research scholarship PQ to the first author and CAPES for the Master scholarship to the second author.

References

[1] I. Dincer, M.A. Rosen, Thermal Energy Storage (Systems and Applications), Wiley, 2002.
[2] S.A. Formin, T.S. Saitoh, Melting of unfixed material in spherical capsule with non-isothermal wall, Int. J. Heat Mass Transfer 42 (1999) 4197–4205.
[3] M. Bareiss, H. Beer, An analytical solution of the heat transfer process during melting of an unfixed solid phase change material inside a horizontal tube, Int. J. Heat Mass Transfer 27 (1999) 739–746.
[4] J. Caldwell, C.C. Chan, Spherical solidification by enthalpy method and the heat balance integral method, Appl. Math. Model. 24 (2000) 45–53.
[5] K.A.R. Ismail, J.R. Henriquez, Solidification of PCM inside a spherical capsules, Energy Convers. Manage. 41 (2000) 173–187.
[6] J.M. Khodadadi, Y. Zhang, Effects of buoyancy-driven convection on melting within spherical containers, Int. J. Heat Mass Transfer 44 (2001) 1605–1618.
[7] I. Eames, K.T. Adref, Freezing and melting of water in spherical enclosures of the type used in thermal (ice) storage system, Appl. Therm. Eng. 22 (2002) 733–745.
[8] A. Barba, M. Spiga, Discharge mode for encapsulated PCMs in storage tanks, Solar Energy 74 (2003) 141–148.
[9] K.A.R. Ismail, J.R. Henriquez, T.M. Silva, A parametric study on ice formation inside a spherical capsule, Int. J. Therm. Sci. 42 (2003) 881–887.
[10] L. Bilir, Z. Ilken, Total solidification time of liquid phase material enclosed in cylindrical/spherical containers, Appl. Therm. Eng. 25 (2005) 1488–1502.
[11] T. Kouskson, J.-P. Bédécarrats, J.-P. Dumas, A. Mimet, Dynamic modeling of the storage of an encapsulated ice tank, Appl. Therm. Eng. 25 (2005) 1534–1548.
[12] J. Wei, Y. Kawagushi, S. Hirano, H. Takeuchi, Study on a PCM heat storage system for rapid heat supply, Appl. Therm. Eng. 25 (2005) 2903–2920.
[13] Z.A. Hammou, M. Lacroix, A hybrid thermal energy storage system for managing simultaneously solar and electric energy, Energy Convers. Manage. 47 (2006) 273–288.
[14] N. Yuksel, A. Avci, M. Kilic, A model for latent heat energy storage systems, Int. J. Energy Res. 30 (2006) 1146–1157.
[15] H. Ettouney, I. Alatiqi, M. Al-Sahalil, K. Al-Hajirie, Heat transfer enhancement in energy storage in spherical capsules filled with paraffin wax and metal beads, Energy Convers. Manage. 47 (2006) 211–228.
[16] E. Assis, L. Katsman, G. Ziskind, R. Letan, Numerical and experimental study of melting in a spherical shell, Int. J. Heat Mass Transfer 50 (2007) 1790–1804.
[17] K.A.R. Ismail, Bancos de gelo, Fundamentos e modelagem, State University of Campinas, Campinas, Unicamp, SP, Brasil, 1998, ISBN 85-900609-2-6.
[18] K.A.R. Ismail, Modelagem e processos térmicos; Fusão e solidificação, State University of Campinas, Unicamp, Campinas, SP. Brasil, 1998, ISBN 85-900609-3-4.